# Optimal bone strength and mineralization requires the type 2 iodothyronine deiodinase in osteoblasts

J. H. Duncan Bassett[a], Alan Boyde[b], Peter G. T. Howell[b,c], Richard H. Bassett[d], Thomas M. Galliford[a], Marta Archanco[a], Holly Evans[e], Michelle A. Lawson[e], Peter Croucher[e], Donald L. St. Germain[f], Valerie Anne Galton[f], and Graham R. Williams[a,1]

[a]Molecular Endocrinology Group, Division of Medicine and Medical Research Council Clinical Sciences Centre, Imperial College London, Hammersmith Hospital, London W12 0NN, United Kingdom; [b]Oral Growth and Development, Institute of Dentistry, Bart's and London School of Medicine, Queen Mary University of London, London E1 1BB, United Kingdom; [c]Division of Restorative Dental Sciences, Eastman Dental Institute, and [d]Department of Civil and Environmental Engineering, University College London, London WC1E 6BT, United Kingdom; [e]The Mellanby Centre for Bone Research, Department of Human Metabolism, University of Sheffield, Sheffield S10 2RX, United Kingdom; and [f]Departments of Physiology and Medicine, Dartmouth Medical School, Lebanon, NH 03756

Edited by Peter K. Vogt, The Scripps Research Institute, La Jolla, CA, and approved March 18, 2010 (received for review October 1, 2009)

**Hypothyroidism and thyrotoxicosis are each associated with an increased risk of fracture. Although thyroxine (T4) is the predominant circulating thyroid hormone, target cell responses are determined by local intracellular availability of the active hormone 3,5,3′-L-triiodothyronine (T3), which is generated from T4 by the type 2 deiodinase enzyme (D2). To investigate the role of locally produced T3 in bone, we characterized mice deficient in D2 (D2KO) in which the serum T3 level is normal. Bones from adult D2KO mice have reduced toughness and are brittle, displaying an increased susceptibility to fracture. This phenotype is characterized by a 50% reduction in bone formation and a generalized increase in skeletal mineralization resulting from a local deficiency of T3 in osteoblasts. These data reveal an essential role for D2 in osteoblasts in the optimization of bone strength and mineralization.**

thyroid hormone metabolism | fracture | hypothyroidism | bone formation | skeleton

Thyroid hormones are essential for linear growth and peak bone mass acquisition. In adults, thyrotoxicosis results in high bone turnover osteoporosis and increased susceptibility to fracture, whereas hypothyroidism reduces bone turnover (1–3). In previous studies, we identified thyroid hormone receptor α (TRα) as the critical mediator of 3,5,3′-L-triiodothyronine (T3) action in bone (4–7). The aim of this study is to investigate the role of the type 2 iodothyronine deiodinase (D2) as a local prereceptor modulator of T3 action in the skeleton.

Thyroid hormone actions are determined by local availability of T3 to its nuclear receptor (8). D2 catalyzes removal of an outer ring 5′-iodine atom from the major circulating hormone thyroxine (T4) to generate the active metabolite T3. Conversely, the type 3 deiodinase (D3) inactivates both T4 and T3 by removal of an inner ring 5-iodine atom. Thus, D2 and D3, in conjunction with serum-derived T3, are important local modulators of thyroid hormone action in vivo. Expression of D2 and D3 is regulated in a temporo-spatial and tissue-specific manner, resulting in varying levels of T3 action in individual tissues despite relatively constant serum thyroid hormone levels (8).

Mice deficient in D2 (D2KO) exhibit pituitary resistance to feedback regulation by T4 characterized by a 3-fold increase in serum thyroid-stimulating hormone (TSH), a 27% increase in the serum T4 level, but a normal T3 level. The increased TSH and T4 levels are evident as early as postnatal day (PD)10 (9). These changes are accompanied by cold intolerance, impaired hearing, and reduced brain T3 content (10). The type 1 deiodinase (D1) is widely believed to catalyze conversion of T4 to T3 in tissues such as liver and kidney, predominantly for export to plasma. Like the D2KO mice, D1/D2KO double-mutant mice exhibit increases in serum T4 and TSH and have a normal serum T3 level (10).

The roles of D1 and D2 in regulating T3 action in the skeleton have not been studied, although limited information regarding growth is available. A minor and transient impairment of weight gain was reported in male D2KO mice, whereas weight gain and growth were normal in D1KO and D1-deficient C3H/HeJ mice and in C3H/HeJ D2KO mutants with D1 and D2 deficiency (11–15). We and others have shown that D1 is not expressed in skeletal cells (16–19), indicating D1 does not influence T3 action in bone directly. D2 activity has been demonstrated in the embryonic growth plate where it is regulated by the skeletal morphogen Hedgehog (20). Nevertheless, D2 activity was not identified in primary chondrocytes, growth plate tissue extracts, or primary organ cultures from postnatal animals (19, 21–23), suggesting a discrete role during embryonic development. In osteoblasts data are conflicting (16, 18, 24), although specific D2 activity was identified in whole bone and differentiated MC3T3 osteoblastic cells in one study (17). Using a sensitive and highly specific HPLC-based assay, we showed D2 is restricted to mature primary osteoblasts but is undetectable in chondrocytes and osteoclasts (19). We hypothesized, therefore, that D2KO and D1/D2KO mice would display equivalent abnormalities of bone turnover and mineralization reflecting the restricted activity of D2 in mature osteoblasts and the absence of D1 from bone.

## Results

**D2KO Mice Have Brittle Bones.** The strength and biomechanical characteristics of bone from adult D2KO and D1/D2KO mice were investigated by destructive three-point bend testing (Fig. 1 *A* and *B*). Analysis of load displacement curves revealed the extrinsic rigidity (stiffness), intrinsic stiffness (Young's modulus), and biomechanical parameters of WT and mutant bones to be similar (Fig. 1 *B* and *C i-ii*, Fig. S1, and Table S1). The major difference in mutant femurs was their behavior following maximum load. WT specimens showed considerable work softening, demonstrated by a 35% fall in applied load from 18.4 ± 0.8 N to 12.2 ± 1.2 N, whereas displacement continued to 0.43 ± 0.03 mm before fracture occurred (Fig. 1*C iii–iv*, Fig. S1, and Table S1). By contrast, mutant femurs sustained a sudden fracture almost immediately after maximum load (Fig. S1). Thus, femurs from mutant mice behave as a classic brittle material that fails in a single abrupt fracture. WT femurs, however, sustain nonpropagating microfractures that absorb energy but do not result in failure until considerable internal microdamage has occurred. The major benefits of these nonpropagating microfractures are that

Author contributions: J.H.D.B., V.A.G., and G.R.W. designed research; J.H.D.B., A.B., T.M.G., M.A., H.E., M.A.L., V.A.G., and G.R.W. performed research; D.L.S.G. and V.A.G. contributed new reagents/analytic tools; J.H.D.B., A.B., P.G.T.H., R.H.B., H.E., M.A.L., P.C., and G.R.W. analyzed data; and J.H.D.B. and G.R.W. wrote the paper.

The authors declare no conflict of interest.

This article is a PNAS Direct Submission.

[1]To whom correspondence should be addressed. E-mail: graham.williams@imperial.ac.uk.

This article contains supporting information online at www.pnas.org/cgi/content/full/0911346107/DCSupplemental.

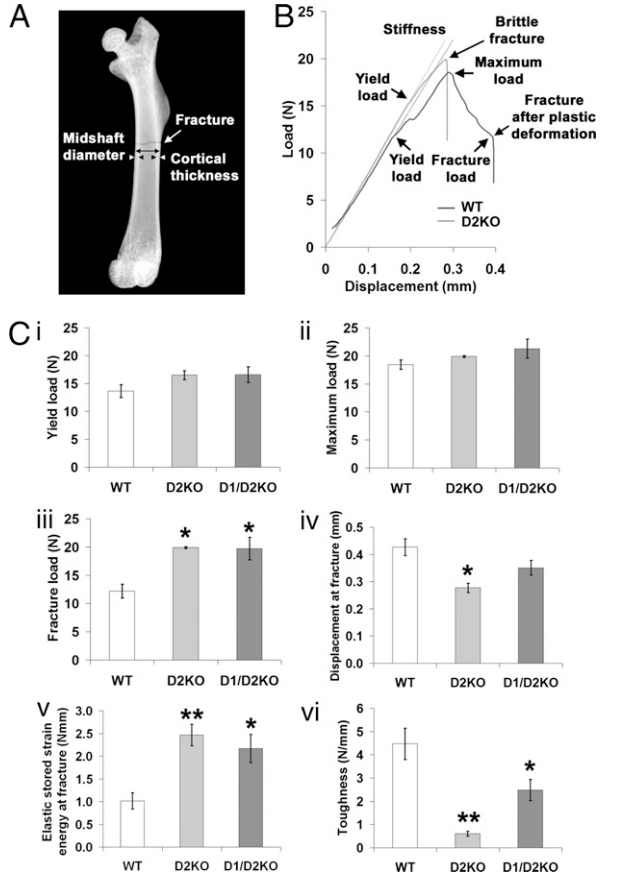


**Fig. 1.** Mechanical properties of bone in D2KO and D1/D2KO mice. (*A*) Faxitron image of fractured femur following a three-point bend test. The site of fracture and region for measurement of diameter and cortical thickness are shown. (*B*) Load–displacement curves of WT and D2KO femurs. The points of yield load, maximum load, and fracture load and the gradient of the linear elastic phase, representing the extrinsic rigidity or stiffness of the bone, are shown. (*C*) Graphs showing (*i*) yield load, (*ii*) maximum load, (*iii*) fracture load, (*iv*) displacement at fracture, (*v*) elastic stored-strain energy at fracture, and (*vi*) toughness of WT, D2KO, and D1/D2KO femurs. ANOVA and Tukey's post hoc test; *, $P < 0.05$, **, $P < 0.01$ versus WT (n = 5–7).

the bone can survive marked deformation beyond maximum load and significant elastic stored-strain energy is dissipated before fracture. Thus, only a small amount of stored energy remains at final fracture, resulting in less widespread damage. The elastic stored-strain energy at maximum load and fracture is illustrated in Fig. S1. At maximum load, values in bones of both WT and mutant mice were similar, but at fracture the value in WT femurs had fallen by 79%, the remaining stored energy being only 1.0 Nmm compared with 2.5 Nmm in D2KO mice (Fig. 1*Cv*, Table S1, Fig. S1). Indeed, the mutant femurs dissipated only 21–46% of their energy before fracture (Table S1). Thus, WT bones display work-softening ductility, whereas femurs from D2KO mice are brittle, have reduced toughness, and sustain destructive fractures (Fig. 1*Cvi*, Table S1).

**High Bone Mineral Density and Osteoblast-Specific Hypothyroidism in D2KO Mice.** To determine whether brittle bones in D2KO mice result from abnormal mineralization, bone mineral density was measured by Faxitron point projection digital microradiographic analysis and quantitative backscattered electron scanning electron microscopy (qBSE-SEM). Relative and cumulative frequency histograms obtained from Faxitron analysis of tibias revealed increased bone mineral content in mutant mice (Fig. 2*A* and *B*). Detailed studies at the cubic-micrometer volume resolution scale were performed using qBSE-SEM. Frequency histograms of bone micromineralization densities from combined cortical and trabecular bone sites (Fig. S2*A* and *B*) or discrete regions of trabecular (Fig. 2 *C* and *D*) and cortical (Fig. 2 *E* and *F*) bone demonstrated high bone mineralization in mutants. Further studies were performed to determine whether these findings were recapitulated by manipulation of systemic thyroid status in WT mice. A similar increase in bone mineral content was observed in hypothyroid mice, whereas bone mineral content was reduced in thyrotoxic animals (Fig. S3). Thus, in addition to brittle bones, adult D2KO mice have increased bone mineralization consistent with tissue hypothyroidism in bone, despite a normal circulating level of T3. To investigate further, in situ hybridization

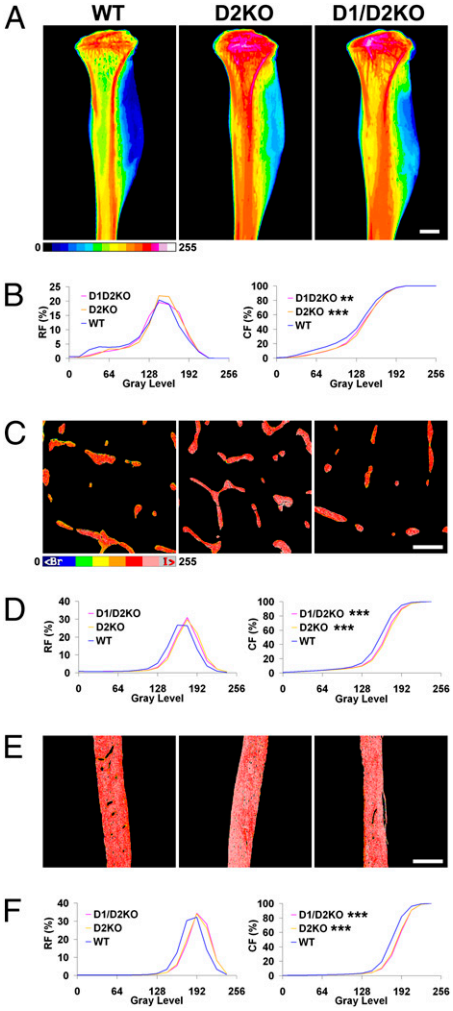


**Fig. 2.** Bone micromineralization density in D2KO and D1/D2KO mice. (*A*) Faxitron images of tibias from PD112 WT, D2KO, and D1/D2KO mice. Gray-scale images were pseudocolored according to a 16-color palette; low mineralization density is black, high density is white. (Scale bar, 1 mm.) (*B*) Relative (RF) and cumulative frequency (CF) histograms of mineralization densities from whole tibia. Kolmogorov-Smirnov test; **, $P < 0.01$; ***, $P < 0.001$ versus WT ($n$ = 5–6). (*C*) qBSE-SEM images of metaphyseal trabecular bone from PD112 WT, D2KO, and D1/D2KO mice. (Scale bar, 200 μm.) Gray-scale images were pseudocolored according to an eight-color palette; low mineralization density is blue, high density is gray. Regions of trabecular bone correspond to boxed areas in Fig. S2*A*. (Scale bar, 200 μm.) (*D*) RF and CF histograms of trabecular bone micromineralization densities from femur, tibia, and humerus. Kolmogorov-Smirnov test; ***, $P < 0.001$ versus WT ($n$ = 4). (*E*) qBSE-SEM images of midshaft humerus cortical bone. (*F*) RF and CF histograms of cortical bone micromineralization densities from femur, tibia, and humerus. Kolmogorov-Smirnov test; ***, $P < 0.001$ versus WT ($n$ = 4).

was performed to determine expression of the T3-target gene *Fgfr1* in bone. These studies revealed an osteoblast-specific reduction in *Fgfr1* expression in mutant mice, indicating the presence of restricted cellular hypothyroidism in osteoblasts (Fig. S4).

**Normal Bone Development in D2KO Mice.** Skeletal development was analyzed to determine whether this phenotype results from abnormal bone formation and growth. There were no differences in skeletal elements between mutant and WT mice at PD1. Bone formation and growth did not differ between PD14 and PD112, and treatment of WT and D2KO mice with T3 had no effect (Fig. 3 and Fig. S5). Histological analysis of the tibia revealed a 20% reduction in total growth plate height in PD21 D1/D2KO mice compared with WT, but no differences were found in D2KO mice or mice treated with T3 (Fig. 3 *D–F*). The reduced growth plate height in D1/D2KO mice resulted from narrower reserve (RZ) and hypertrophic (HZ) zones, and small reductions in the heights of the proliferative zone (PZ) and HZ were evident in D2KO mice.

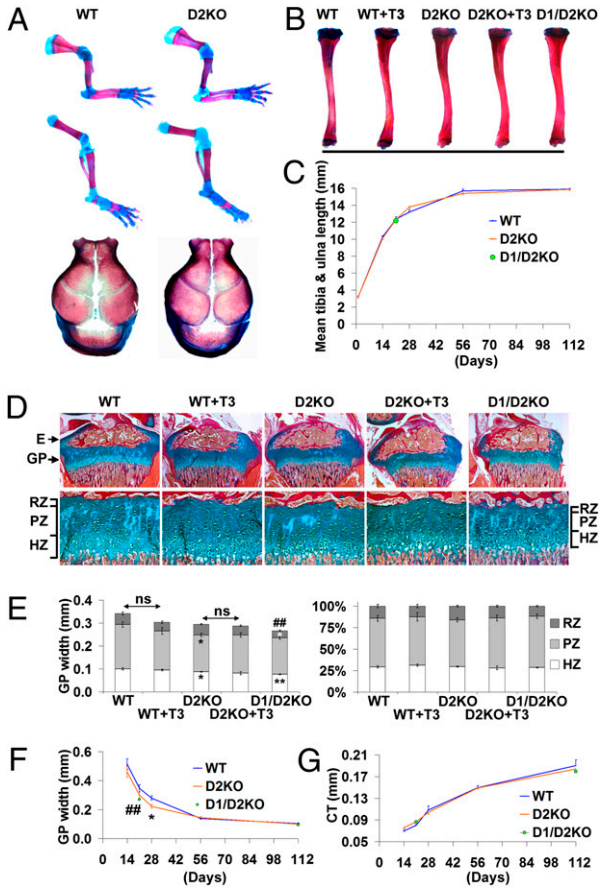


**Fig. 3.** Bone development and growth in D2KO and D1/D2KO mice. (*A*) Limbs and skull from PD1 WT and D2KO mice stained with Alcian blue (cartilage) and alizarin red (bone). (*B*) Tibias from PD21 WT, WT+T3-treated, D2KO, D2KO+T3-treated, and D1/D2KO mice. (*C*) Growth curves between birth and PD112. ($n$ = 4–14). (*D*) Proximal tibia growth plates stained with Alcian blue and van Gieson (osteoid) (magnification ×50 and ×200). E, epiphysis; GP, growth plate; HZ, hypertrophic zone; PZ, proliferative zone; RZ, reserve zone. (*E*) Growth plate and chondrocyte zone heights in PD21 mice. Growth plate zone measurements (*Left*) and proportions relative to height of the growth plate (*Right*). ANOVA and Tukey's post hoc test, D2KO and D1/D2KO versus WT: *, $P < 0.05$; **, $P < 0.01$ comparison of growth plate zones; ##, $P < 0.01$ comparison of growth plate heights ($n$ = 4–8). (*F*) Changes in growth plate heights between PD14 and PD112. Student's $t$ test: *, $P < 0.05$ D2KO versus WT; ##, $P < 0.01$ D1/D2KO versus WT ($n$ = 3–8). (*G*) Changes in femur cortical bone thickness (CT) between PD14 and PD112 ($n$ = 3–5).

Nevertheless, the relative sizes of the RZ, PZ, and HZ were similar in all genotypes, and growth plate parameters did not differ in PD56 and PD112 mice, indicating that any difference was minor and transient. Importantly, the differences were not accompanied by altered linear growth or bone formation and are thus of no biological significance. Similarly, cortical bone thickness did not differ in mutant or T3-treated mice (Fig. 3*G* and Fig. S5 *C* and *D*). The normal endochondral ossification in D2KO mice is consistent with the absence of D2 activity in growth plate chondrocytes (19), and the adult brittle bone phenotype therefore is not a consequence of abnormal skeletal development.

**Normal Bone Microarchitecture but Reduced Bone Volume in D2KO Mice.** To determine whether brittle bones and increased mineralization were accompanied by structural changes of the adult skeleton, bone microarchitecture was analyzed by BSE-SEM. Low-power views of distal femur (Fig. 4*A*) revealed no differences in cortical bone thickness and trabecular bone structure between mutant and WT mice. In-high power views (Fig. 4*B*), the thickness and connectivity of individual trabeculae were similar also. Thus, adult mutant mice have normal bone microarchitecture. The bone volumes of vertebrae and long bones (BV/TV) were determined by qBSE-SEM and high-

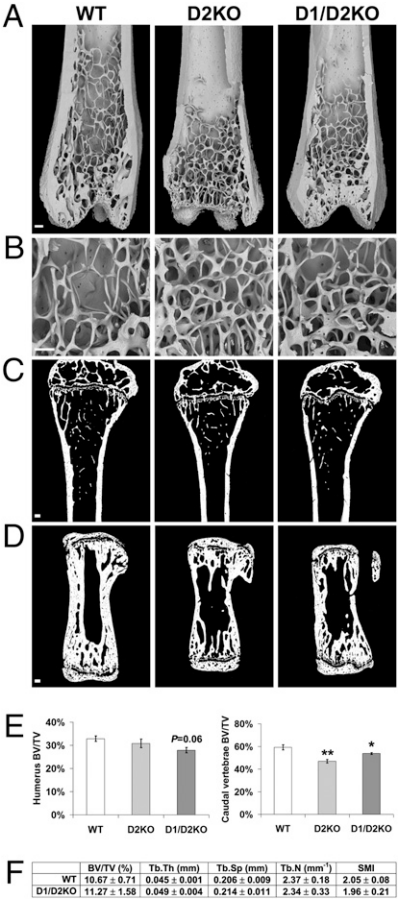


| | BV/TV (%) | Tb.Th (mm) | Tb.Sp (mm) | Tb.N ($mm^{-1}$) | SMI |
|---|---|---|---|---|---|
| WT | 19.67 ± 0.71 | 0.045 ± 0.001 | 0.206 ± 0.009 | 2.37 ± 0.18 | 2.05 ± 0.08 |
| D1/D2KO | 11.27 ± 1.58 | 0.049 ± 0.004 | 0.214 ± 0.011 | 2.34 ± 0.33 | 1.96 ± 0.21 |

**Fig. 4.** Bone microarchitecture in D2KO and D1/D2KO mice. (*A* and *B*) BSE-SEM views of distal femur from PD112 WT, D2KO, and D1/D2KO mice. (Scale bars, 200 μm.) (*C* and *D*) Sections of proximal humerus and caudal vertebra from PD112 WT, D2KO, and D1/D2KO mice imaged by qBSE SEM. (Scale bars, 200 μm.) (*E*) Quantitative analysis of bone volume (BV/TV) in PD112 mice. ANOVA and Tukey's post hoc test. *, $P < 0.05$; **, $P < 0.01$ versus WT ($n$ = 4). (*F*) Trabecular bone volume (BV/TV), trabecular thickness (Tb.Th), trabecular spacing (Tb.Sp), trabecular number (Tb.N), and structure model index (SMI) determined by micro-CT analysis of proximal tibia from PD112 D1/D2KO and WT mice ($n$ = 5).

resolution micro-CT (Fig. 4 *C–F*). Vertebral bone volume was reduced by 20% in D2KO mice ($P < 0.01$) and by 9% in D1/D2KO mice ($P < 0.05$), whereas long bone parameters were similar.

**Normal Bone Resorption in D2KO Mice.** To investigate whether altered bone resorption accounts for the brittle bone phenotype, the numbers of osteoclasts (Oc.N), osteoclast surfaces (Oc.S), and total bone surfaces (BS) were quantified (Fig. 5 *A* and *B*). There were no differences in Oc.N/BS or Oc.S/BS in mutant mice, indicating that osteoclast numbers and resorption were normal. To investigate further, areas of scalloped osteoclast bone resorption on endosteal and trabecular bone surfaces were quantified by BSE-SEM (Fig. 5 *C–E*). There was no difference in the resorption surface relative to total bone surface, confirming that bone resorption is normal in mutant mice. Accordingly, there were no differences in the serum bone resorption markers C-terminal crosslinked telopeptide of type I collagen (CTX) and tartrate-resistant acid phosphatase form 5b (TRAP) (Fig. S6). Thus, the phenotype is not a consequence of altered bone resorption.

**Reduced Bone Formation in D2KO Mice.** To investigate whether altered osteoblastic bone formation accounts for the phenotype, mineralizing surfaces, BS, mineral apposition rates (MAR), and bone formation rates (BFR) were quantified in calcein double-labeled adult mice (Fig. 6 *A–D*). In mutants mineralizing surfaces were reduced by 25–35% in trabecular bone and 45–46% in calvaria, whereas MAR was reduced by 17–28% in trabecular bone and 24–36% in calvaria. Consequently, BFR was reduced by 37–52% in trabecular bone and by 58–72% in calvaria. Histomorphometric analysis of trabecular osteoblast function was performed also (Fig. 6 *E* and *F*). Osteoblast surfaces (Ob.S) and number (Ob.N) and osteoid surfaces (OS) and width (O.Wi) were quantified. Ob.S/BS was reduced by 43–56% in mutant mice, whereas Ob.N/Ob.S was increased by 29–38%. Consequently, the total number of osteoblasts (Ob.N/BS) did not differ between WT and mutant mice, although mutant osteoblasts were smaller (Fig. 6*F*). Osteoid surface per mm of osteoblast surface (OS/Ob.S) also was similar in all animals, but O.Wi was reduced by 39–49% in mutants. Although the BFR was decreased in mutant mice, serum bone formation markers were not reduced at PD91, reflecting the low levels of bone turnover markers observed at this age and the greater sensitivity of dynamic histomorphometry (Fig. S6). Thus, the brittle bone phenotype in D2KO mice results from reduced osteoblast activity.

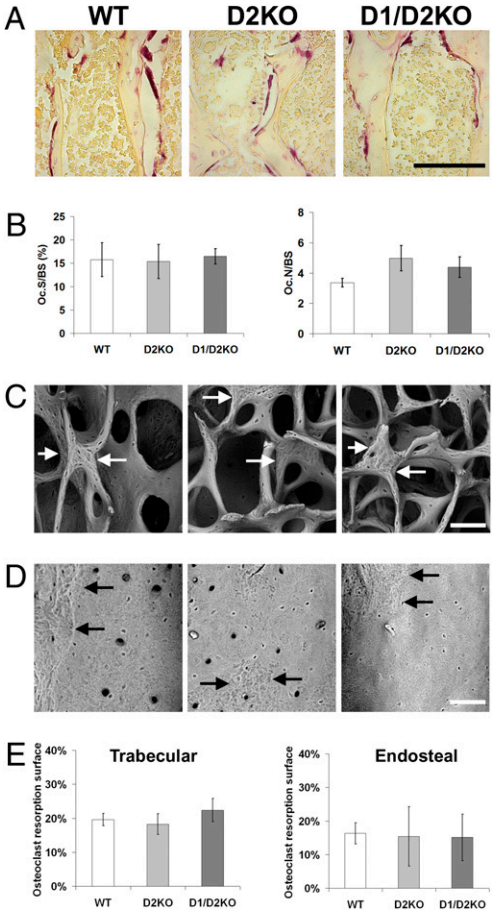


**Fig. 5.** Bone resorption in D2KO and D1/D2KO mice. (*A*) TRAP-stained sections from PD112 WT, D2KO, and D1/D2KO mice. (Scale bar, 100 μm.) (*B*) Quantitative analysis of osteoclast surface (Oc.S) and the number of TRAP-positive osteoclasts (Oc.N) relative to bone surface (BS). ANOVA ($n = 3–4$). (*C*) Trabecular bone surfaces from PD112 WT, D2KO, and D1/D2KO mice imaged by BSE-SEM. White arrows indicate roughened osteoclast resorption surfaces. (Scale bar, 200 μm.) (*D*) Endosteal surfaces from PD112 mice. Black arrows indicate junctions between roughened resorption surfaces and smooth unresorbed bone. (Scale bar, 200 μm.) (*E*) Quantitative analysis of osteoclast resorption surfaces (% of total bone surface). ANOVA ($n = 3–5$).

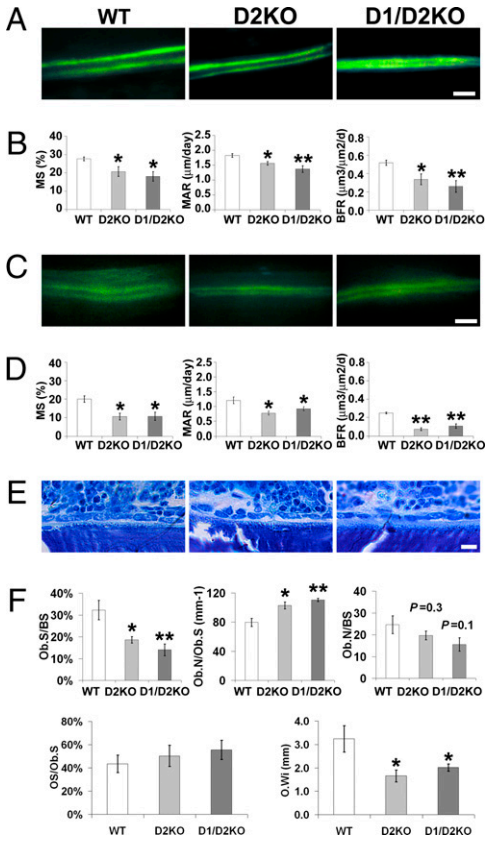


**Fig. 6.** Bone formation in D2KO and D1/D2KO mice. (*A*) CSLM views of trabecular bone. (Scale bar, 10 μm.) (*B*) Trabecular bone mineralizing surface (MS), mineral apposition rate (MAR), and bone formation rate (BFR) determined by dual calcein labeling. ANOVA and Tukey's post hoc test; *, $P < 0.05$; **, $P < 0.05$ versus WT ($n = 4$). (*C*) CSLM views of calvarial bone. (Scale bar, 10 μm.) (*D*) Quantitative analysis of intramembranous bone deposition in calvaria. *, $P < 0.05$ versus WT; **, $P < 0.05$ versus WT ($n = 3–4$). (*E*) Toluidine blue-stained osteoblasts from PD112 WT, D2KO, and D1/D2KO mice. (Scale bar, 10 μm.) (*F*) Histomorphometry analysis of osteoblast parameters. *, $P < 0.05$ versus WT; **, $P < 0.05$ versus WT ($n = 4$).

## Discussion

We demonstrate that D2KO mice, which lack D2 that regulates intracellular T3 availability, have brittle bones of increased mineralization and reduced bone formation because of restricted cellular hypothyroidism in osteoblasts. These data provide fundamental insight into thyroid hormone action in bone, revealing an essential role for D2 in optimizing toughness and mineralization of the skeleton.

**D2 Is Essential for Normal Osteoblast Function.** Studies of the skeletal consequences of hypothyroidism in humans demonstrated low bone turnover and a prolonged bone remodeling cycle with impaired osteoclast and osteoblast function (25–27). Osteoclast activity and bone resorption surfaces were reduced, and osteoblast activity and osteoid apposition were impaired. The bone formation phase in each remodeling cycle was prolonged 4-fold, resulting in an extended period of secondary mineralization (25–27). In the current studies, D2KO mice similarly had low bone turnover and impaired osteoblast activity with reduced mineralized surfaces and BFR. Osteoclast function was unaffected, indicating D2KO mice have an osteoblast-specific defect that results from intracellular T3 deficiency despite the presence of a normal circulating concentration of T3. This phenotype is consistent with restricted expression *Dio2* in osteoblasts and its absence from osteoclasts (19). D1/D2KO mice exhibited a phenotype comparable with D2KO mice, reflecting the absence of D1 activity in bone (16–19). Thus, reduced toughness and resistance to fracture in D2KO and D1/D2KO mice reveals an important role for D2 in osteoblasts in the optimization of bone strength.

**Mouse Models of Skeletal Hypo- and Hyperthyroidism.** Recent studies in congenitally hypothyroid TSH receptor-null mice have proposed TSH as a regulator of bone turnover acting directly in osteoblasts and osteoclasts (28). Further in vivo studies demonstrated increased bone formation and reduced bone resorption in rats and mice treated with doses of TSH that were insufficient to affect circulating thyroid hormone levels (29). The current findings, however, are inconsistent with these observations, because D2KO and D1/D2KO mice exhibit impaired rather than increased bone formation and normal rather than reduced bone resorption despite a 3-fold elevation of the serum TSH level and a normal serum T3 concentration. Thus, the role of TSH in bone remains uncertain (30).

By contrast, the importance of D2 activity in osteoblasts is supported by the skeletal phenotypes of thyroid receptor (TR)-mutant mice. $TR\alpha1^{R384C/+}$ mice, which express a dominant negative TRα1 protein, have skeletal hypothyroidism because of impaired TRα1 signaling in bone that results in increased bone mineralization and an additional reduction in osteoclast activity (4). $TR\beta^{-/-}$ mice have central thyroid hormone resistance, elevated serum thyroid hormone levels, and skeletal hyperthyroidism caused by increased activation of TRα1, the predominant TR isoform in bone. Accordingly, this skeletal hyperthyroidism results in reduced bone mineralization and increased osteoclast activity (4, 5). Together, these data indicate that defective TRα1 signaling inhibits osteoblast and osteoclast activities, whereas increased activation of TRα1 stimulates both osteoblasts and osteoclasts. In D2KO and D1/D2KO mice, however, the cellular defect is different, because D2 activity normally is present only in osteoblasts. D2KO and D1/D2KO mutants lack intracellular D2-mediated T4 to T3 conversion but have a normal circulating T3 concentration. Thus, cellular hypothyroidism in bone is restricted to osteoblasts and consequently is manifest by reduced bone formation and increased mineralization without an accompanying defect of osteoclast function. The normal physiological activity of TRα1 in osteoblasts therefore requires an adequate intracellular level of T3 that is dependent, at least in part, on D2. By contrast, thyroid hormones and TRα1 also exert D2-independent actions in osteoclasts.

Thyroid status, therefore, influences the activities of both osteoclasts and osteoblasts. Thyrotoxicosis increases osteoblast and osteoclast activities, resulting in high bone turnover osteoporosis (2), whereas hypothyroidism results in low bone turnover with reduced osteoblast and osteoclast activities and a net increase in bone mineralization (25–27). Surprisingly, large population studies demonstrate that both conditions are associated with an increased susceptibility to fracture (3, 31, 32).

**D2 Has an Essential Physiological Role in Bone.** The current study identifies a critical function for D2 in osteoblasts that may account for this unexpected observation. The findings suggest a model in which restricted expression of D2 maintains a higher intracellular T3 concentration in osteoblasts relative to other skeletal cells that is essential for their normal function (Fig. 7*A*). An analogous role for D2 has been described previously in the developing cochlea (33). As in other tissues, D2 activity in osteoblasts is up-regulated in hypothyroidism and down-regulated in hyperthyroidism (17). Thus, D2 acts as a local homeostatic regulator that buffers the detrimental effects of altered serum thyroid hormone levels on the skeleton. We propose that adverse effects of T3 deficiency on bone mineralization are mitigated by increased D2-mediated conversion of T4 to T3 in osteoblasts, whereas inhibition of osteoblastic D2 activity limits the detrimental effects of thyroid hormone excess. Nevertheless, the capacity of this local feedback mechanism in osteoblasts is insufficient to compensate in overt hypothyroidism or thyrotoxicosis (Fig. S3). Thus, we hypothesize that optimal bone mineral content and resistance to fracture are maintained over the physiological range of systemic thyroid hormone concentrations by the regulated activity of D2 in osteoblasts (Fig. 7*B*). Absence of this compensatory mechanism in D2KO mice results in cellular hypothyroidism and brittle bones. These

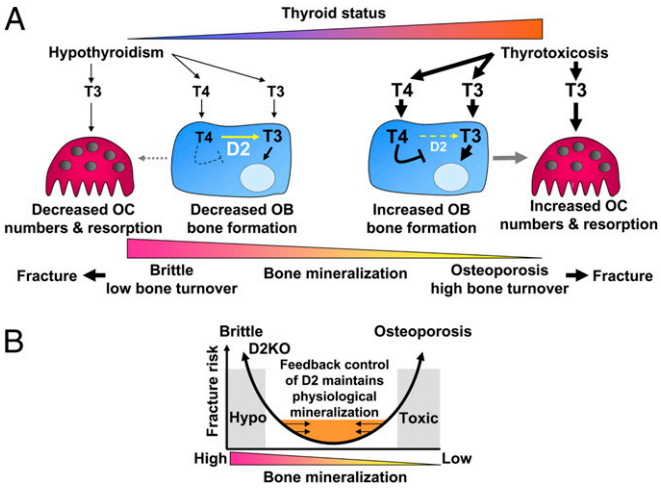


**Fig. 7.** Proposed physiological role for D2 in bone. (*A*) Thyroid status regulates osteoclasts (OC) and osteoblasts (OB). Hypothyroidism reduces bone turnover and thyrotoxicosis increases bone turnover, but both conditions increase fracture risk. In osteoblasts, D2 is up-regulated in hypothyroidism but is reduced in hyperthyroidism. We propose that increased D2-mediated conversion of T4 to T3 in osteoblasts mitigates adverse effects of T3 deficiency on bone mineralization, whereas reduced osteoblastic D2 activity limits the detrimental effects of thyroid hormone excess. (*B*) Role of D2 in the relationship between bone mineralization and fracture risk. Regulated D2 activity in osteoblasts maintains optimal bone mineralization within the euthyroid range. Absence of this local feedback mechanism in D2KO mice results in cellular hypothyroidism despite circulating euthyroidism, an isolated reduction in osteoblast activity, and brittle bones. The system, however, has insufficient capacity to compensate in overt hypothyroidism and thyrotoxicosis, resulting in increased susceptibility to fracture in both conditions.

studies identify D2 as a possible therapeutic target to manipulate bone strength.

## Materials and Methods

**D2KO and D1/D2KO Mice.** Homozygous colonies of WT, D2KO, and D1KO mice were housed at Dartmouth Medical School animal facility using protocols approved by the Institutional Review Board. Some PD21 mice were rendered hyperthyroid by adding T3 (0.3 μg/mL) to the drinking water of nursing mothers (*SI Materials and Methods*).

**Faxitron Imaging.** Digital x-ray images of long bones and tail vertebrae at 10-μm resolution were recorded using a Qados Faxitron MX20 variable kV point projection x-ray source (Cross Technologies plc.) (*SI Materials and Methods*).

**qBSE-SEM.** Bone micromineralization densities were analyzed at cubic-micrometer resolution by qBSE-SEM (*SI Materials and Methods*).

**Mechanical Testing.** Three-point bend tests were performed on femurs from PD112 mice using an Instron 5543 load frame (Instron Limited) (*SI Materials and Methods*).

**Skeletal Preparations and Histology.** PD1 mice and limbs from older animals were stained with alizarin red and Alcian blue. Sections of decalcified bones were stained with van Gieson and Alcian blue, and growth plate and cortical bone dimensions were determined. Osteoclasts were analyzed in sections stained for TRAP (*SI Materials and Methods*).

**BSE-SEM.** Long bones were fixed in 70% ethanol, opened longitudinally, cleaned of cell remnants, and imaged by BSE-SEM (*SI Materials and Methods*).

**Micro-CT Analysis.** Tibia were fixed and stored in 70% ethanol and subsequently imaged by microCT at a detection pixel size of 4.3 $\mu m^2$. (*SI Materials and Methods*).

**Measurement of Bone Turnover Markers.** Serum markers of bone formation and resorption were measured in samples from P91 WT and D1D2KO mice (*SI Materials and Methods*).

**Confocal Microscopy.** Midline longitudinal and midcoronal block faces were cut through methacrylate-embedded long bones and calvaria. Specimens were examined by confocal autofluorescence scanning light microscopy (CSLM) to determine the fraction of bone surface undergoing active bone formation (*SI Materials and Methods*).

**Osteoblast Histomorphometry.** Methacrylate embedded sections were stained with toluidine blue, and primary histomorphometric indices of bone formation were determined (*SI Materials and Methods*).

**ACKNOWLEDGMENTS.** We thank Maureen Arora for SEM studies. The work was supported by a Medical Research Council (MRC) Clinician Scientist Fellowship (to J.H.D.B.), a grant from the Horserace Betting Levy Board (to A.B.), and MRC Research and Wellcome Trust Project grants (to G.R.W.). The scanning electron microscope was funded by the MRC.

1. Mosekilde L, Eriksen EF, Charles P (1990) Effects of thyroid hormones on bone and mineral metabolism. *Endocrinol Metab Clin North Am* 19:35–63.
2. Murphy E, Williams GR (2004) The thyroid and the skeleton. *Clin Endocrinol (Oxf)* 61: 285–298.
3. Vestergaard P, Rejnmark L, Mosekilde L (2005) Influence of hyper- and hypothyroidism, and the effects of treatment with antithyroid drugs and levothyroxine on fracture risk. *Calcif Tissue Int* 77:139–144.
4. Bassett JH, et al. (2007) Thyroid status during skeletal development determines adult bone structure and mineralization. *Mol Endocrinol* 21:1893–1904.
5. Bassett JH, et al. (2007) Thyroid hormone excess rather than thyrotropin deficiency induces osteoporosis in hyperthyroidism. *Mol Endocrinol* 21:1095–1107.
6. O'Shea PJ, et al. (2005) Contrasting skeletal phenotypes in mice with an identical mutation targeted to thyroid hormone receptor alpha1 or beta. *Mol Endocrinol* 19: 3045–3059.
7. O'Shea PJ, et al. (2003) A thyrotoxic skeletal phenotype of advanced bone formation in mice with resistance to thyroid hormone. *Mol Endocrinol* 17:1410–1424.
8. Bianco AC, Kim BW (2006) Deiodinases: Implications of the local control of thyroid hormone action. *J Clin Invest* 116:2571–2579.
9. Galton VA, et al. (2007) Thyroid hormone homeostasis and action in the type 2 deiodinase-deficient rodent brain during development. *Endocrinology* 148:3080–3088.
10. Galton VA, Schneider MJ, Clark AS, St Germain DL (2009) Life without thyroxine to 3,5,3′-triiodothyronine conversion: Studies in mice devoid of the 5′-deiodinases. *Endocrinology* 150:2957–2963.
11. Schneider MJ, et al. (2001) Targeted disruption of the type 2 selenodeiodinase gene (DIO2) results in a phenotype of pituitary resistance to T4. *Mol Endocrinol* 15: 2137–2148.
12. Berry MJ, et al. (1993) Physiological and genetic analyses of inbred mouse strains with a type I iodothyronine 5′ deiodinase deficiency. *J Clin Invest* 92:1517–1528.
13. Schneider MJ, et al. (2006) Targeted disruption of the type 1 selenodeiodinase gene (Dio1) results in marked changes in thyroid hormone economy in mice. *Endocrinology* 147:580–589.
14. Schoenmakers CH, Pigmans IG, Poland A, Visser TJ (1993) Impairment of the selenoenzyme type I iodothyronine deiodinase in C3H/He mice. *Endocrinology* 132: 357–361.
15. Christoffolete MA, et al. (2007) Mice with impaired extrathyroidal thyroxine to 3,5,3′-triiodothyronine conversion maintain normal serum 3,5,3′-triiodothyronine concentrations. *Endocrinology* 148:954–960.
16. Dreher I, et al. (1998) Selenoproteins are expressed in fetal human osteoblast-like cells. *Biochem Biophys Res Commun* 245:101–107.
17. Gouveia CH, et al. (2005) Type 2 iodothyronine selenodeiodinase is expressed throughout the mouse skeleton and in the MC3T3-E1 mouse osteoblastic cell line during differentiation. *Endocrinology* 146:195–200.
18. LeBron BA, Pekary AE, Mirell C, Hahn TJ, Hershman JM (1989) Thyroid hormone 5′-deiodinase activity, nuclear binding, and effects on mitogenesis in UMR-106 osteoblastic osteosarcoma cells. *J Bone Miner Res* 4:173–178.
19. Williams AJ, et al. (2008) Iodothyronine deiodinase enzyme activities in bone. *Bone* 43:126–134.
20. Dentice M, et al. (2005) The Hedgehog-inducible ubiquitin ligase subunit WSB-1 modulates thyroid hormone activation and PTHrP secretion in the developing growth plate. *Nat Cell Biol* 7:698–705.
21. Ballock RT, Reddi AH (1994) Thyroxine is the serum factor that regulates morphogenesis of columnar cartilage from isolated chondrocytes in chemically defined medium. *J Cell Biol* 126:1311–1318.
22. Böhme K, Conscience-Egli M, Tschan T, Winterhalter KH, Bruckner P (1992) Induction of proliferation or hypertrophy of chondrocytes in serum-free culture:The role of insulin-like growth factor-I, insulin, or thyroxine. *J Cell Biol* 116:1035–1042.
23. Wakita R, Izumi T, Itoman M (1998) Thyroid hormone-induced chondrocyte terminal differentiation in rat femur organ culture. *Cell Tissue Res* 293:357–364.
24. Morimura T, et al. (2005) Expression of type 2 iodothyronine deiodinase in human osteoblast is stimulated by thyrotropin. *Endocrinology* 146:2077–2084.
25. Eriksen EF, Mosekilde L, Melsen F (1986) Kinetics of trabecular bone resorption and formation in hypothyroidism: Evidence for a positive balance per remodeling cycle. *Bone* 7:101–108.
26. Melsen F, Mosekilde L (1980) Trabecular bone mineralization lag time determined by tetracycline double-labeling in normal and certain pathological conditions. *Acta Pathol Microbiol Scand [A]* 88:83–88.
27. Mosekilde L, Melsen F (1978) Morphometric and dynamic studies of bone changes in hypothyroidism. *Acta Pathol Microbiol Scand [A]* 86:56–62.
28. Abe E, et al. (2003) TSH is a negative regulator of skeletal remodeling. *Cell* 115: 151–162.
29. Sun L, et al. (2008) Intermittent recombinant TSH injections prevent ovariectomy-induced bone loss. *Proc Natl Acad Sci USA* 105:4289–4294.
30. Bassett JH, Williams GR (2008) Critical role of the hypothalamic-pituitary-thyroid axis in bone. *Bone* 43:418–426.
31. Vestergaard P, Mosekilde L (2002) Fractures in patients with hyperthyroidism and hypothyroidism: A nationwide follow-up study in 16,249 patients. *Thyroid* 12: 411–419.
32. Ahmed LA, Schirmer H, Berntsen GK, Fønnebø V, Joakimsen RM (2006) Self-reported diseases and the risk of non-vertebral fractures: The Tromsø study. *Osteoporos Int* 17: 46–53.
33. Ng L, et al. (2004) Hearing loss and retarded cochlear development in mice lacking type 2 iodothyronine deiodinase. *Proc Natl Acad Sci USA* 101:3474–3479.